Light Scattering from Glass-forming Molten Salts

A. G. Kalampounias[a,b], G. N. Papatheodorou[a,b], and S. N. Yannopoulos[a]

[a] Foundation for Research and Technology Hellas – Institute of Chemical Engineering and High Temperature Chemical Processes, P.O. Box 1414, GR-26500 Patras, Greece

[b] Department of Chemical Engineering, University of Patras, GR-26500, Patras, Greece

Reprint requests to Dr. S. N. Y; Fax: +30 61 965 223, E-mail: sny@iceht.forth.gr

Z. Naturforsch. **57 a,** 65–70 (2002); received August 20, 2001

Presented at the NATO Advanced Study Institute, Kas, Turkey, May 4 - 14, 2001.

Raman scattering has been employed to study the temperature and polarization dependence of the vibrational modes for the glass-forming halide salt mixtures $x\mathrm{ZnCl_2}$-$(1-x)\mathrm{AlCl_3}$, with x = 0.8 and 0.6. The analysis has shown that the vibrational modes of the mixtures arise from a contribution of the vibrational modes of the pure components salts. Emphasis has also been given to the low-frequency modes (3 - 80 cm^{-1}), and particular points related to the glass transition phenomenology are discussed in view of the experimental findings.

Key words: Halide Glasses; Molten Salts; Raman Scattering; Glass Transition; Boson Peak.

1. Introduction

Despite the intense efforts and the immense body of experimental and theoretical data accumulated, glass transition is considered as the least understood phase transition in condensed matter physics [1 - 3]. The liquid to glass transition is a many body problem, complicated further by nonlinear interactions between the constituent particles, and as such the establishment of a theoretical basis that can qualitatively and quantitatively treat it correctly is a formidable task. The problem with which a glass transition theory is faced stems from the observed phenomenology that supercooled liquids display similar / ubiquitous features, although with subtle differences, irrespective of their chemical nature. Thus, chemically disparate substances with (i) strong covalent bonds, like oxide glasses, (ii) hydrogen bonds, like alcohols, (iii) non-directional van der Waals bonds, like polymers and (iv) ionic interactions, like molten salts, are found among molecular and macromolecular glass formers.

The role played by molten salts in the elucidation of the not yet clarified issues of the glass transition is quite significant. Their simpler structure compared with the polymeric or other multi-component glasses is the major advantage that often facilitates the interpretation of the dynamical features in terms of structural models. Halide, and especially chloride glass forming salts are maybe the less studied systems due to the inherent difficulties they present during their purification procedure. $\mathrm{ZnCl_2}$ is an exception that has been given attention by many research works, and therefore its structural and dynamical properties are to a great extent known [4, 5]. However, $\mathrm{ZnCl_2}$ ($T_\mathrm{g} \approx$ 102 °C, $T_\mathrm{m} \approx 320$ °C) has the disadvantage of presenting a broad crystallization region (ca. 170 - 260 °C) within the supercooled range, inaccessible to the experiment. A long time ago it has been appreciated that the addition of $\mathrm{AlCl_3}$ to pure $\mathrm{ZnCl_2}$ results in a softening of the zinc chloride network, enhancing the glass forming ability of the binary systems [6]. Contrary to the behaviour of pure $\mathrm{ZnCl_2}$, in the binary glasses up to 40% moles concentration in $\mathrm{AlCl_3}$ one can continuously scan the supercooled range and monitor in detail changes in both structure and dynamics.

In this work we have undertaken a light scattering (Raman) investigation in order to probe particular aspects of some not yet fully understood topics pertaining to the glass transition phenomenology.

2. Experimental

Anhydrous $\mathrm{ZnCl_2}$ (Alfa, ultra pure) was used after distillation and filtering under vacuum through a high porosity quartz frit. Anhydrous $\mathrm{AlCl_3}$ (Alfa, reagent grade) was used after four repeated sublimations, the

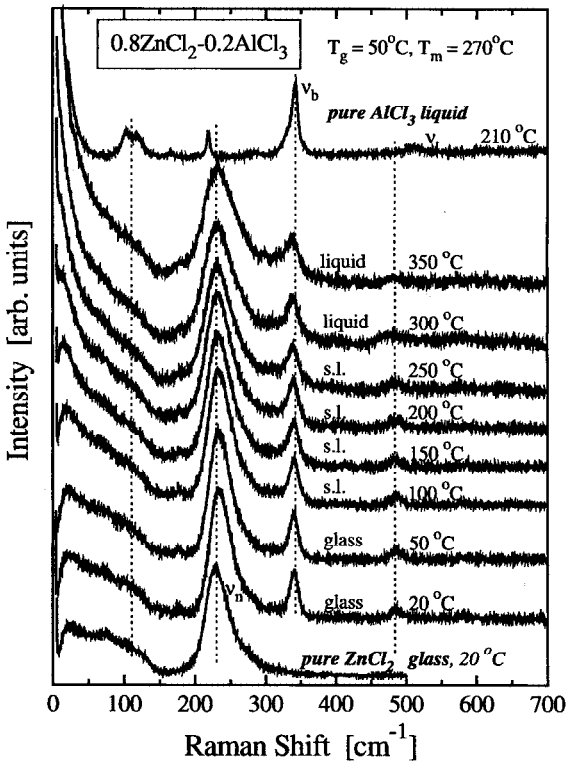

Fig. 1. Representative Stokes-side Raman spectra of the $0.8ZnCl_2$-$0.2AlCl_3$ mixture in the glassy, supercooled and molten state. The spectra of the pure $ZnCl_2$ glass and the $AlCl_3$ melt are also shown for comparison. (s.l. = supercooled liquid).

first through a quartz frit with high porosity also. Due to their hygroscopic nature, the treatment of chemicals has been performed in an inert-gas filled glove box, and the glasses have been prepared through moderate cooling into evacuated silica tubes (6 mm o.d. - 4 mm i.d.). The mixtures corresponding to the desired molar ratios were kept ~100 °C above their melting points and then quenched at room temperature. The prepared glasses were colorless, transparent and free of any cracks. The glass transition temperature for the $x = 0.8$ composition has been found to be $T_g \approx 50$ °C while for the $x = 0.6$ glass, $T_g \approx 15$ °C [7].

Right angle spectra were recorded by a 0.85 m double monochromator (Spex 1403). The excitation source was an Ar^+ laser operating with an output power 200 mW at 488 nm. The instrumental resolution was fixed at 1.5 cm^{-1} for the whole set of measurements, and the temperature was controlled with an accuracy of ±1 K. Both scattering geometries, polarized (VV) and depolarized (HV), were employed and a calibration procedure with the aid of a Neon lamp was often taking place in order correct for possible drifts of the monochromator's gratings. Spectra were recorded for the glass, the supercooled liquid and the melt with small temperature steps.

3. Results and Discussion

3.1. High-frequency Modes – Short-range Structure

Temperature dependent studies are quite common when studying glass-forming liquids. This has proved useful because temperature variations facilitate the elucidation of structure, and often structural models are proposed based on the temperature dependence of the intensity, width, polarization, frequency shift etc. for particular vibrational lines. However, since the population of the energy levels involved in the scattering process depends on temperature, one should be able to disentangle the changes brought about to the vibrational lines due to temperature and due to alterations of local species equilibria or modifications in structure. This is usually done by means of the so-called reduction procedures. According to the Boson-like statistical description of phonons, the mean number of phonons at a particular temperature is given by $n(\omega, T) = [\exp(\hbar\omega/k_B T) - 1]^{-1}$, where $\hbar$ and k_B are Planck's and Boltzmann's constants, respectively. Therefore, the Stokes-side reduced Raman spectrum reads as

$$I^{red}(\omega) = (\omega_L - \omega)^{-4}\omega[n(\omega, T) + 1]I^{exp}(\omega), \quad (1)$$

where the term in the forth power is the usual correction for the wavelength dependence of the scattered intensity.

Representative Raman spectra in the "raw" and reduced form are shown for the $0.8ZnCl_2$-$0.2AlCl_3$ system in Figs. 1 and 2, respectively. The spectra of the pure salts $ZnCl_2$ (glass) and $AlCl_3$ (liquid) are also presented in Figure 1. Apart from changes in the relative intensities the overall spectra and band positions for the mixture with $x = 0.6$ were similar to those with $x = 0.8$.

Aluminum chloride forms a molecular liquid consisting of Al_2Cl_6 dimers (Fig. 3a). The high intensity band observed in the spectra $\nu_b = 342$ cm^{-1} (Fig. 1) has been attributed to the Al-Cl-Al bridging mode, while the high frequency band $\nu_t = 530$ cm^{-1} is due to the Al-Cl terminal stretching frequency [8]. The

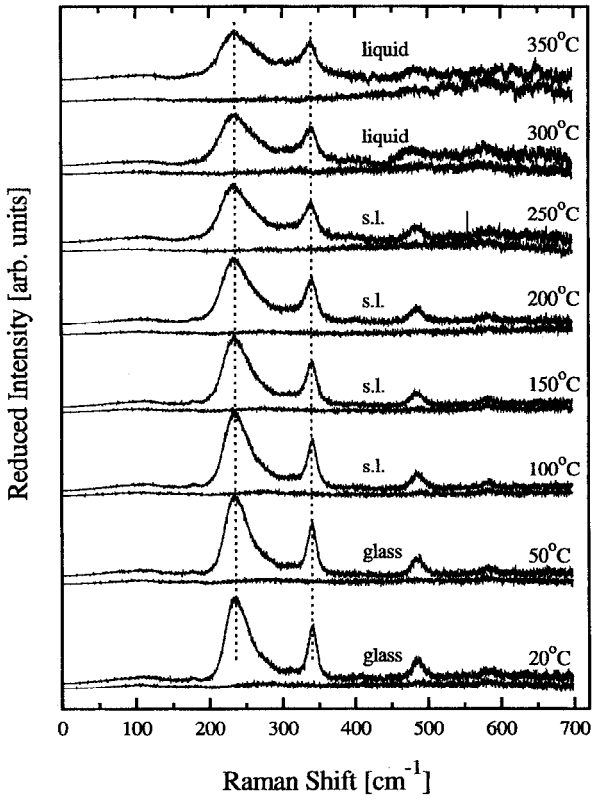

Fig. 2. Reduced form – according to (1) – of the spectra presented in Figure 1.

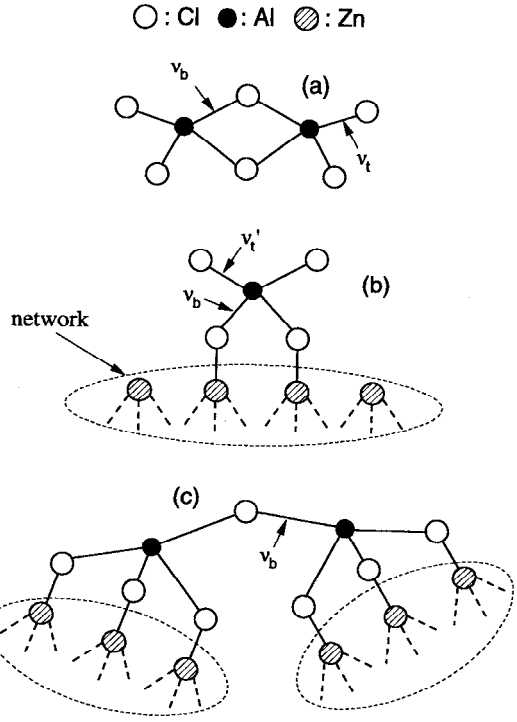

Fig. 3. Schematic representation of the Al_2Cl_6 dimer (a), and two possible ways of aluminum chloride incorporation into the zinc chloride network (b) and (c). In form (b) an $AlCl_4^-$ tertahedron originating from the dimer breaking may be attached either on the surface of a cluster of the $ZnCl_2$ network or in higher concentration might disrupt the network structure. On the other hand, in conformations of the (c) form, the $Al_2Cl_7^-$ ion acts as soft connector between adjacent isolated clusters.

strongest broad band for pure glassy or molten $ZnCl_2$ is at $\nu_n = 228$ cm^{-1} (Fig. 1) and has been attributed to the bridged Zn-Cl stretching vibration at the $ZnCl_4$ "tetrahedra" participating in the $ZnCl_2$ network [9].

The spectra of the mixture (Figs. 1 and 2) at frequencies above 200 cm^{-1} appear to be a superposition of the spectra of the individual components showing both the aluminum chloride ν_b and ν_t and the zinc chloride ν_n bands. At frequencies below 200 cm^{-1} the spectra of the mixture are dominated by the Boson peak and the low frequency vibrations of $ZnCl_2$, while the bending modes of the Al_2Cl_6 dimer vanish in the mixture.

The fact that the ν_b bridging frequency does not seem to change in the mixture leads to the conclusion that the Al_2Cl_6 dimer does not substantially dissociate nor experience strong interactions with the surroundings in the $ZnCl_2$ rich molten mixtures [6]. However the presence of molecular like Al_2Cl_6 in the network (solvent) of $ZnCl_2$ is questionable. As discussed in the introduction, the addition of $AlCl_3$ in $ZnCl_2$ enhances the glass forming ability of the binary system which indirectly implies that $AlCl_3$ contributes to the stabilization of the network. Therefore a possible explanation of the appearance of the ν_b peak intensity in the mixtures can be visualized by invoking the presence of bridging chlorides between the aluminum and zinc atoms participating in the network.

Two such cases are shown in Fig. 3 (b) and (c). In case (b) the $AlCl_4^-$ "tetrahedra" created by splitting the dimer (a) are bound by two bridging chlorides to the $ZnCl_2$ network, while in case (c) an $Al_2Cl_7^-$ like structure [10] bridges an aluminum atom both to another aluminum and to the $ZnCl_2$ network. In the dimer (a) the aluminum atoms compete for the bridging chloride, while in the structures (b) and (c) the competition is between aluminum and two or more zinc atoms participating in the network. Assuming

that in both cases the competition is energetically similar, we would expect the bridging frequency ν_b not to change as we go from the liquid aluminum chloride to the mixture where structures like (b) and (c) are formed.

The terminal ν_t stretching frequency in the dimer shows a shift to lower energies in the $ZnCl_2$-$AlCl_3$ mixtures (ν_t'), which implies that the electronic density of the terminal chlorides is pulled towards the bridging band (Fig. 3b) and enhances the bonding between the aluminum atom and the network.

The main peaks of $ZnCl_2$ ν_n and of $AlCl_3$ ν_b remain at the same energy in going from the glass to the melt, see Figure 2. They both broaden as the temperature increases, however almost maintaining the ratio of their intensities. This last finding implies that the temperature does not alter drastically the network and that the ν_b and ν_n bands cannot be ascribed to individual species in chemical equilibrium.

The main peak of the pure $ZnCl_2$ $\nu_n = 228$ cm^{-1} has a shoulder band in the region 260 - 280 cm^{-1} which has been considered to arise from polynuclear $(ZnCl_2)_n$ fragments of smaller size [11]. Further, as the content of the $AlCl_3$ increases, the intensity of the main ν_n peak decreases relative to the $AlCl_3$ ν_b band and shifts to higher frequencies, i.e. it is located at ~234 cm^{-1} for the 80% mixture and at ~241 cm^{-1} for the 60% mixture. A possible cause for this effect is an interaction between $AlCl_3$ and $ZnCl_2$, whereby the polynuclear $(ZnCl_2)_n$ aggregate is being broken up by Al_2Cl_6 molecules resulting in smaller Zn-Cl-Zn aggregates [6].

Finally, it has been recently proposed that, for compositions up to 60 mole% in $ZnCl_2$, Al_2Cl_6 reacts with the $ZnCl_2$ network in the molten state to form terminal $AlCl_2$ units and molecular units of the form $ZnAl_2Cl_8$ in the $AlCl_3$ rich melts [7, 12]. In the $ZnAl_2Cl_8$ molecular unit each Al has two terminal and two bridging Cl. The $AlCl_2$ units decrease the connectivity of the $ZnCl_2$ network, and this has a strong impact on the physical properties of the glasses and melts as shown by the rapidly decreasing glass transition temperature with increasing $AlCl_3$ content.

3.2. *Low-energy Excitations*

In brief, the low-frequency Raman spectrum of amorphous solids and supercooled liquids consist of two contributions that are absent in their crystalline counterparts [13]. Firstly, there is the quasi-elastic

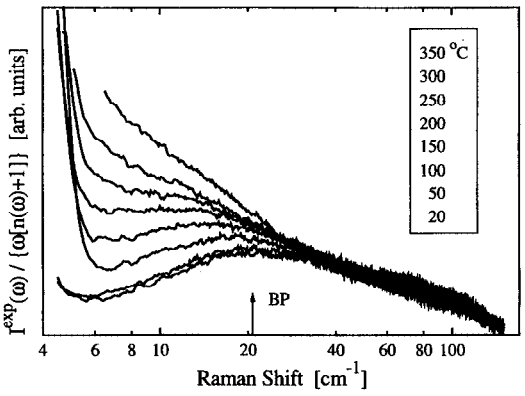

Fig. 4. Semi-log plot of representative Stokes side depolarized low-frequency reduced Raman spectra. The spectra have been scaled (reduced) by the Bose occupation number.

(QE) line that appears in the spectrum as a zero centered line with a half width at half height of about 10 - 15 cm^{-1}; this results in a relaxation time in the sub-picosecond time scale. Secondly, a skew symmetric band, namely the Boson peak, is present with a peak maximum located in the interval 10 - 80 cm^{-1} depending on the material. Numerous putative well-known facts pertaining to the low-frequency Raman phenomenology are currently in dispute [14 - 16].

The spectra presented in Fig. 4 have been scaled with the Bose occupation number $n(\omega, T)$. The remaining temperature dependence reveals the usual behavior, i.e. all the vibrational spectral features that describe first-order scattering coincide after the scaling while the QE line, which originates from anharmonic processes, exhibits a continuous growth. To quantitatively follow the observed changes we have chosen to describe the spectrum by means of a simple theoretical model, which involves the least number of fitting parameters. Therefore, for the analysis of the spectra shown in Fig. 4 we have used a superposition scheme where the QE line is treated as a Lorentzian and the BP is described by the log-normal distribution [17].

Analysis of the experimental data in both polarization geometries is usually overlooked, although the amount of information that can be retrieved is generally critical. Indeed, Fig. 5 depicts the fit at 20 °C conducted to the reduced VV and HV spectra as solid lines. Two low-lying vibrational (optic) modes at ~70 cm^{-1} and ~110 cm^{-1} have also been taken into account for a more reliable determination of the low-frequency components. Global fits have been performed

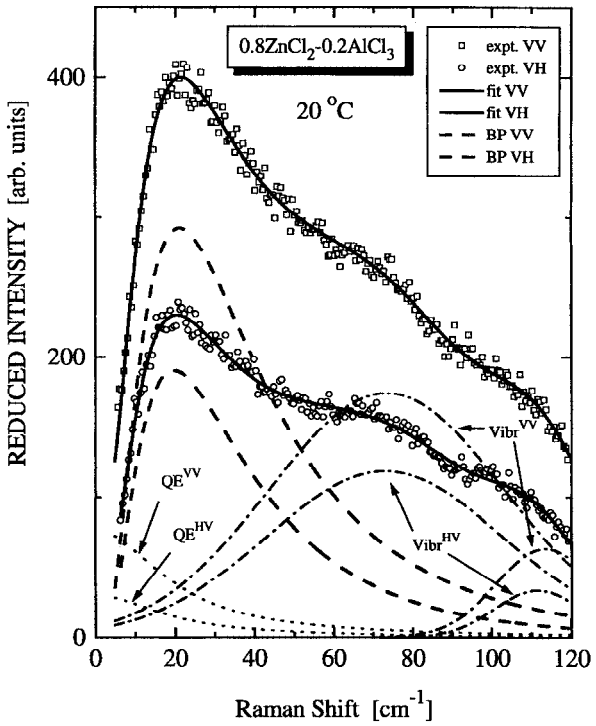

Fig. 5. Polarized (a) and depolarized (b) Stokes side low-frequency reduced Raman spectrum at room temperature. Experimental data are represented by symbols while fits with the superposition model described in the text are shown as continuous lines.

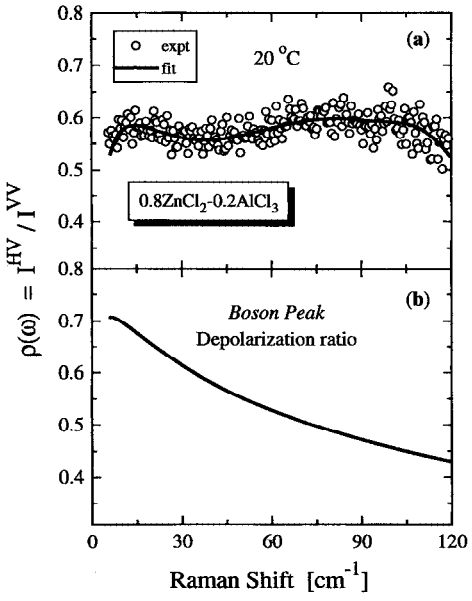

Fig. 6. Frequency dependence of the depolarization ratio in the low-frequency region: (a) total $\rho(\omega)$, (b) partial Boson peak $\rho(\omega)$.

for the two sets (VV and HV) of experimental data. More details will be given in [18].

Let us now turn to the frequency dependence of particular parameters. At first, a successful fitting carried out at both scattering geometries should effectively account for the experimental depolarization ratio. Indeed, as is evident from Fig. 6a, there is a very good agreement between the experimental depolarization ratio (open circles) and the depolarization ratio obtained from the two fitting curves for the room temperature spectrum.

Quite interesting is the outcome revealed when the individual depolarization ratio for the Boson peak is put under focus. While the total depolarization ratio seems almost frequency-independent (although with some particular features), in the case where the individual depolarization ratio is isolated, a clear monotonic decrease is evident, see Figure 6b. This fact is not accidental and is also present for all the temperatures studied. The depolarization ratio starts from the almost highest possible value ($\rho = 3/4$) at very low-frequencies and decreases in a way reminiscent to that predicted by Martin and Brenig (MB) [19]. Independently from the disputes that have occasionally raised about the firm theoretical basis of the MB model, a criterion usually employed for its disapproval has been the putative independence of $\rho(\omega)$ on frequency, see e. g. [20] and [21]. In these works both LiCl-H_2O [20] and the glycerol [21] exhibit broad low-lying optic vibrational modes that significantly affect the scattered intensity down to very low frequencies. Therefore $\rho(\omega)$, that appears as almost constant, is definitely not the depolarization ratio of the pure Boson peak but a composite one with contributions from other vibrational lines.

Frequency dependent depolarization ratios in low-frequency Raman spectra are quite common for many glass-forming liquids [22, 23]. In particular, in [23] it was shown that after disentangling the QE line and the Boson peak, with a procedure that did not require curve fittings, the depolarization ratio for the latter was found to be strongly dependent on frequency. An important conclusion can be drawn from this experimental fact. Specifically, this finding can possibly be explained by considering different distinct mechanisms that may contribute in the frequency range of the Boson peak tail. Interestingly, *ab initio* molecular orbital calculations for glycerol [24] and B_2O_3 [25]

have shown that different vibrational modes are effective within the frequency range of the Boson peak. Such an idea has also been supported in the case of As_2O_3, where the low-frequency Raman spectrum of the crystal exhibits distinct features – each one representing different vibrational mechanism – that conform with the line profile of the low-frequency Raman spectrum of the glass [22].

4. Conclusions

A temperature and polarization dependent Raman scattering study for the $ZnCl_2$-$AlCl_3$ glass-forming mixture has been performed. The high-frequency modes analysis revealed in the mixture the presence of vibrational modes originating from both components. From the temperature and concentration dependence of the vibrational features specific microscopic models, to account for the structure of the mixtures, have been proposed. A joint detailed analysis for both polarized and depolarized spectra in the low-frequency region clearly revealed the frequency dependence of the depolarization ratio; a fact that contradicts the experimental basis on which a particular class of theoretical attempts is erroneously based [26].

[1] See for example the proceedings of the Third International Discussion Meeting on "Relaxations In Complex Systems", ed. by K. L. Ngai, E. Riande, and M. D. Ingram, J. Non-Cryst. Solids 235-237 (1998).
[2] M. D. Ediger, C. A. Angell, and S. R. Nagel, J Phys. Chem. **100**, 13200 (1996).
[3] C. A. Angell, K. L. Ngai, G. B. McKenna, P. F. McMillan, and S. W. Martin, J. Appl. Phys. **88**, 3113 (2000).
[4] E. A. Pavlatou, S. N. Yannopoulos, G. N. Papatheodorou, and G. Fytas, J. Phys. Chem. **101**, 8748 (1997); S. N. Yannopoulos, PhD Thesis, University of Patras, Greece (1996).
[5] C. Dreyfus, M. J. Lebon, F. Vivicorsi, A. Aouadi, R. M. Pick, and H. Z. Cummins, Phys. Rev. E **63**, 041509-1 (2001).
[6] G. M. Begun, J. Brynestad, K. W. Fung, and G. Mamantov, Inorg. Nucl. Chem. Letters **8**, 79 (1972).
[7] S. Petersen, M.-A. Einarsrud, and T. Grande, Proceedings of "The International Terje Ostvold Symposium", Eds. H. A. Oye and O. Waernes, Norway, Nov 2-3, 1998.
[8] T. Tomita, C. E. Sjogren, P. Klaeboe, G. N. Papatheodorou, and E. Rytter, J. Raman Spectrosc. **14**, 415 (1983).
[9] E. A. Pavlatou and G. N. Papatheodorou, in the "Proceedings of the 8th International Symposium on Molten Salts", ed. by R. J. Gale, G. Blomgren, and H. Kojima, The Electrochemical Society Inc., Pennington, Vol. IV **92-16**, 92 (1992).
[10] M. H. Brooker and G. N. Papatheodorou, in "Advances in Molten Salt Chemistry" Vol. 5, ed by G. Mamantov, Elsevier, Amsterdam 1983, pp. 25-184.
[11] D. E. Irish and T. F. Young, J. Chem. Phys. **43**, 1765 (1965).
[12] M.-A. Einarsrud, Ph.D. Thesis, Institute of Inorganic Chemistry, The Norwegian Institute of Technology, Trondheim, Norway, 1987.
[13] J. Jäckle in Amorphous Solids: Low-Temperature Properties, ed. by W. A. Phillips, Springer-Verlag, Berlin 1981, p. 135.
[14] S. N. Yannopoulos and G. N. Papatheodorou, Phys. Rev. B **62**, 3728 (2000).
[15] S. N. Yannopoulos, J. Chem. Phys. **113**, 5868 (2000).
[16] G. N. Papatheodorou and S. N. Yannopoulos, in Proceedings of the NATO-ASI (Kas, Turkey, 4-14 May 2001), Kluwer (2002), Vol. 52.
[17] T. Pang, Phys. Rev. B **45**, 2490 (1992).
[18] A. G. Kalampounias, G. N. Papatheodorou, and S. N. Yannopoulos, J. Non-Cryst. Solids, in press.
[19] A. J. Martin and W. Brenig, Phys. Stat. Solidi (b) **64**, 163 (1974).
[20] N. J. Tao, G. Li, X. Chen, W. M. Du, and H. Z. Cummins, Phys. Rev. A **44**, 6665 (1991).
[21] S. Kojima, Phys. Rev. B **47**, 2914 (1993).
[22] S. N. Yannopoulos, G. N. Papatheodorou, and G. Fytas, J. Chem. Phys. **107**, 1341 (1997).
[23] S. N. Yannopoulos and D. T. Kastrissios, Phys. Rev. E, in press.
[24] T. Uchino and T. Yoko, Science **273**, 480 (1996).
[25] T. Uchino and T. Yoko, J. Chem. Phys. **105**, 4140 (1996).
[26] V. N. Novikov, Phys. Rev. B **58**, 8367 (1998), and references therein.